Heavy Rainfall in Paraguay During the 2015-2016 Austral Summer: Causes and Sub-Seasonal-to-Seasonal Predictive Skill

James Doss-Gollin[1]   Ángel G. Muñoz[2]   Simon J. Mason[2]   Max Pastén[3]

[1]Columbia Water Center, Columbia University [2]International Research Institute for Climate and Society, Columbia University [3]Dirección de Meteorología e Hidrología, Paraguay

Conceptual Framework

Beginning in Nov. 2015, repeated intense rainfall events associated with mesoscale convective activity caused severe flooding along the Paraguay-Paraná river system (fig. 5, red box), displacing over 170 000 people. We use a weather typing approach within a diagnostic framework to show that:

► Moisture and energy advection via the South American Low-Level Jet (SALLJ) [1], particularly during "No-Chaco" events [2] favored mesoscale convective activity
► Strong El Niño and active MJO favored a strong SALLJ but an Atlantic dipole pattern influenced the jet's exit region
► Numerical forecasts predicted enhanced risk of heavy rainfall at the seasonal scale, but biases in spatial patterns suggest difficulties representing Pacific-Atlantic interaction
► Uncorrected sub-seasonal model forecasts of rainfall had limited skill beyond 10-15 days; use of Model Output Statistics – particularly methods that correct both spatial patterns and magnitudes – substantially improved forecast skill

Figure 1: Asunción, Paraguay, 2015-16

Observations and Weather Types

Observations come from:
► Rainfall: CPC Global Unified [3]
► Atmosphere: NCAR-NCEP Reanalysis II [4]
We use weather typing [5] to represent daily circulation patterns:
1. Calculate streamfunction Ψ from meridional and zonal wind [6]
2. Project 850 hPa streamfunction onto leading 4 EOFs
3. K-means clustering using classifiability index [7] to generate a single weather type for each day.

Weather typing simplifies dynamics of daily rainfall but *facilitates analysis of sequences of daily weather patterns.* They are associated with patterns that have been well described in the literature; particularly relevant are:
1. weather type (WT)1 represents "Chaco" jet event [8]
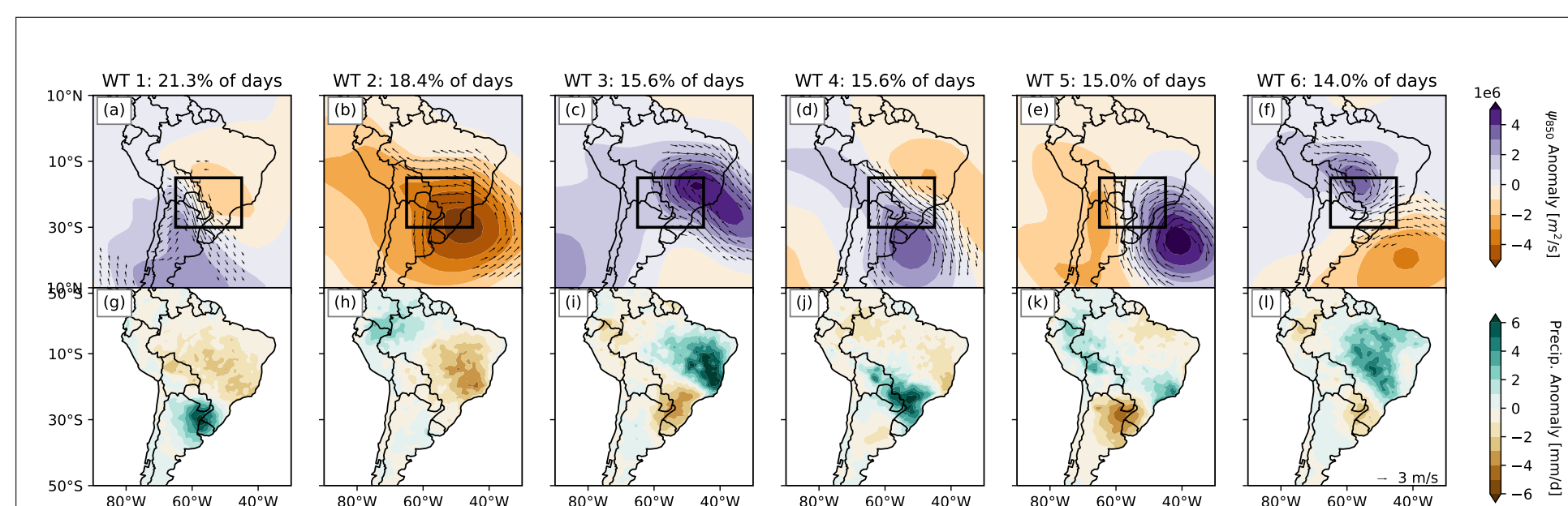2. WT4 represents "No-Chaco" jet events [2]

Figure 2: Composite anomalies associated with each weather type. Top row (a-f) shows streamfunction anomalies at 850 hPa. Strongest 20% of wind anomaly vectors over the plot area are also shown. Bottom row (g-l) shows rainfall anomalies, in units of mm d^{-1}. The relative frequency of occurrence of each weather type (in days) is presented on the top of each column.

Observed Circulation Anomalies

Figure 3: Time series of area-averaged rainfall in the Lower Paraguay River Basin (fig. 5) for each day of NDJF 2015-16. Lines indicate the rainfall value, in units of mm d^{-1}. The weather type corresponding to each day is indicated in an adjacent text label. Dashed lines blue indicate (from bottom to top) the climatological 50th, 90th, and 99th percentiles of NDJF area-averaged rain over the Lower Paraguay River Basin.
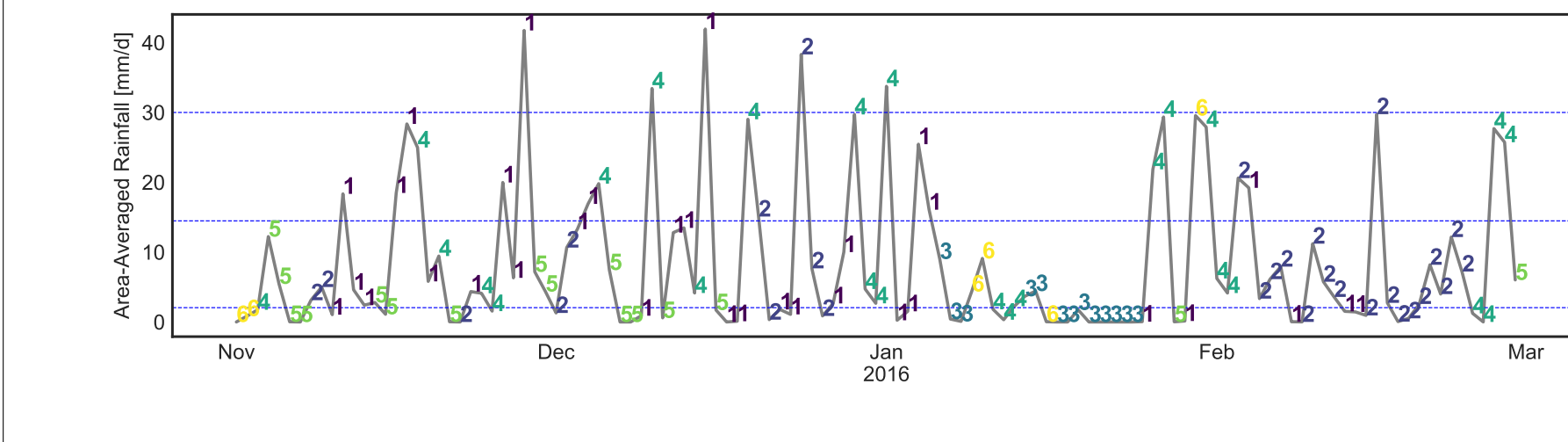
During austral summer (NDJF) 2015-16, most heavy rainfall occurred during WTs 1 and 4 (fig. 3). Monthly-scale circulation anomalies (fig. 4) show a weak anticyclonic circulation that set up over central Brazil during November 2015 and strengthened into the following month. In January 2016 it weakened before returning in February 2016. The observed rainfall and circulation anomalies are consistent with the aggregation of the observed weather types shown in fig. 3.
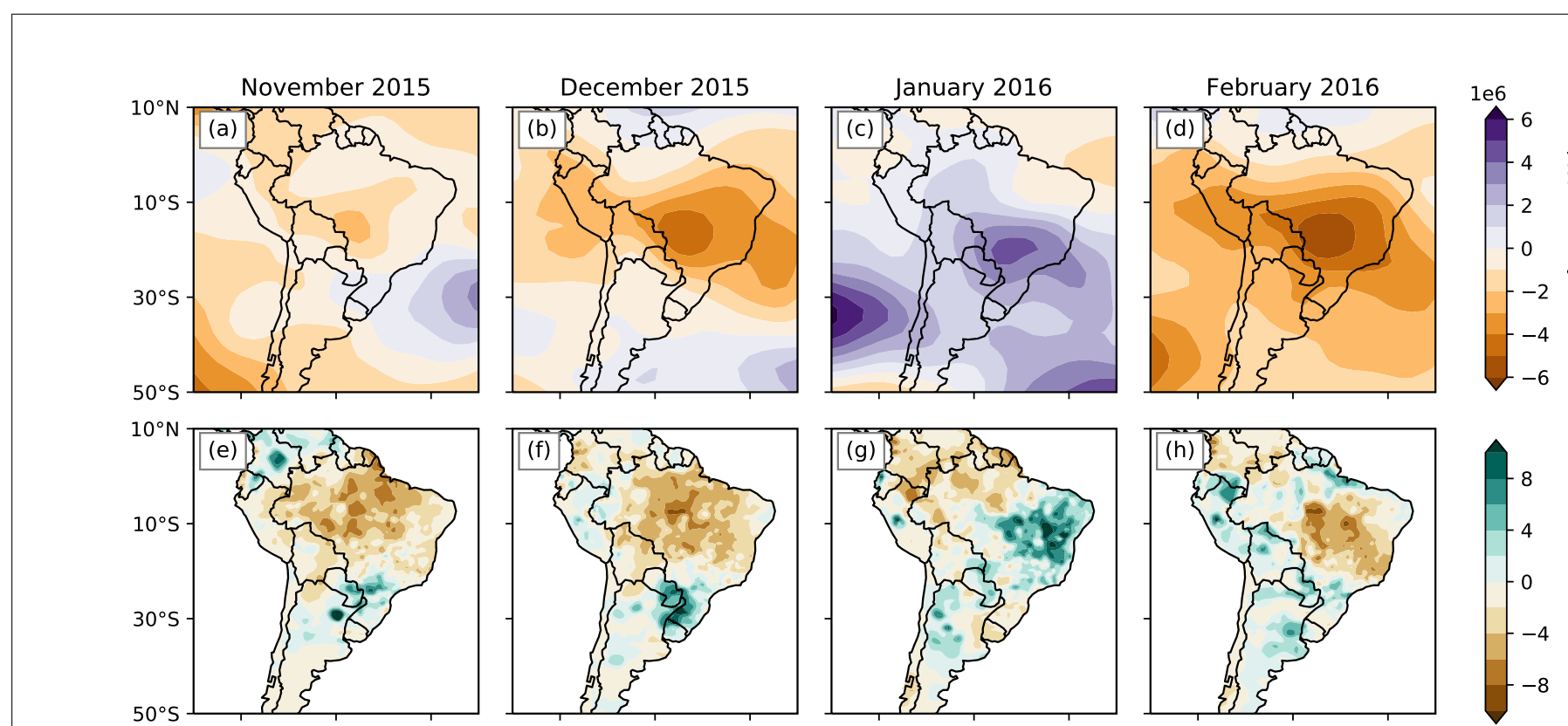

Figure 4: Monthly composite anomalies observed during NDJF 2015-16. Top row shows streamfunction anomalies at 850 hPa. Bottom row shows rainfall anomalies, in units of mm d^{-1}.

Lower Paraguay River Basin

Flat topography limits the river's ability to carry the summer runoff, causing seasonal inundation of the Pantanal and distributing the river discharge in time [9, 10]. During NDJF 2015-16, river stage [height] throughout the Lower Paraguay River Basin reached nearly three times climatological levels (not shown).
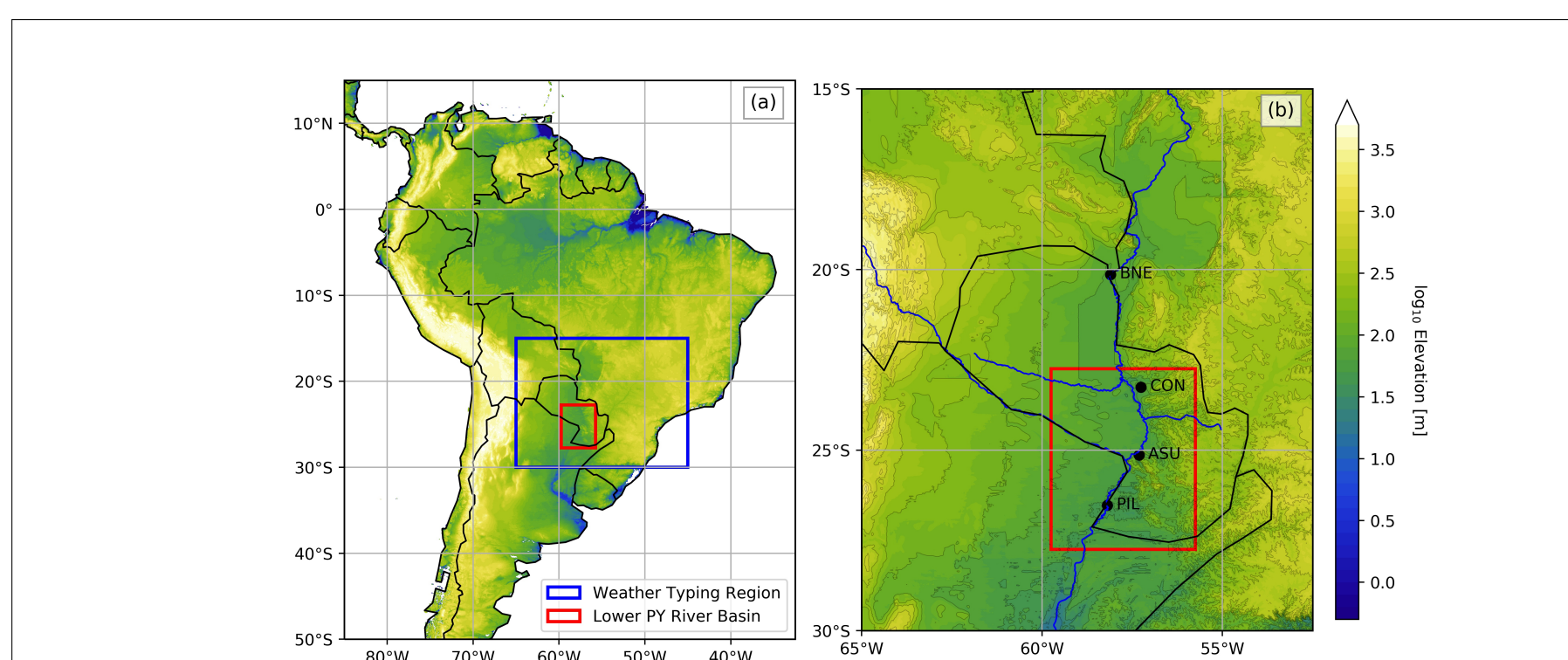

Figure 5: Topographical map of the study area. Colors indicate log$_{10}$ of elevation, in m. (a): all of South America. The domains of the Lower Paraguay River Basin and the domain used for weather typing are indicated in red and blue, respectively. (b): The Lower Paraguay River Basin (LPRB). As for (a), the LPRB is marked with a red box.

S2S Model Forecasts

Figure 6: Chiclet diagram of ensemble-mean precipitation anomaly forecasts over the LPRB from ECMWF S2S forecast data, as a function of the forecast target date (horizontal axis) and lead time (vertical axis). Time series of daily precipitation over the same area is plotted with y-axis inverted.
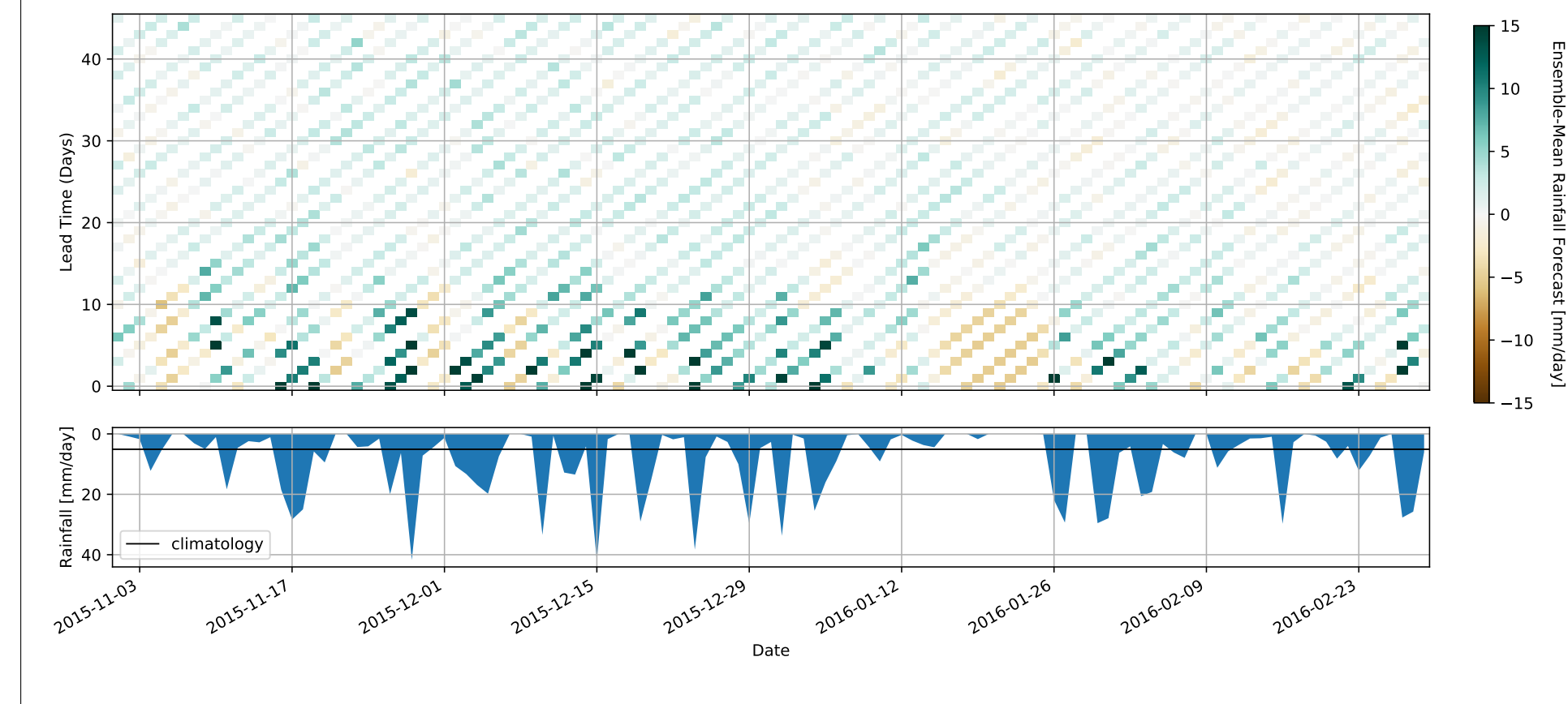

Figure 6 uses a Chiclet diagram [11] to visualize, as a function of lead time, the time evolution of the uncorrected, ensemble-mean rainfall anomaly forecast, spatially averaged over the LPRB. At lead times greater than about two weeks, the ensemble-mean forecast is slightly wetter than climatology. At weather timescales (less than one week), the ensemble-mean successfully predicts the timing and amplitude of the area-averaged rainfall. At intermediate timescales, the model successfully forecast the strongest breaks and pauses in the rainfall, such as the heavy rainfall during December 2015 and the dry period during mid-January 2016.

Model Output Statistics

We explore whether using model output statistics (MOS) [12] can improve the modeled representation of rainfall (fig. 7). Specifically, we use: the raw model output (Raw); homoscedastic extended logistic regression (XLR); heteroscedastic extended logistic regression (HXLR); principal components regression (PCR); and canonical correlation analysis (CCA) using 20 years of ECMWF forecasts. Figure 7 indicates that better forecasts are obtained when both magnitude and spatial corrections are performed (PCR and CCA). The enhanced skill is achieved through the spatial corrections via the EOF-based regressions, which – in contrast with the extended logistic models – use information from multiple grid-boxes,.
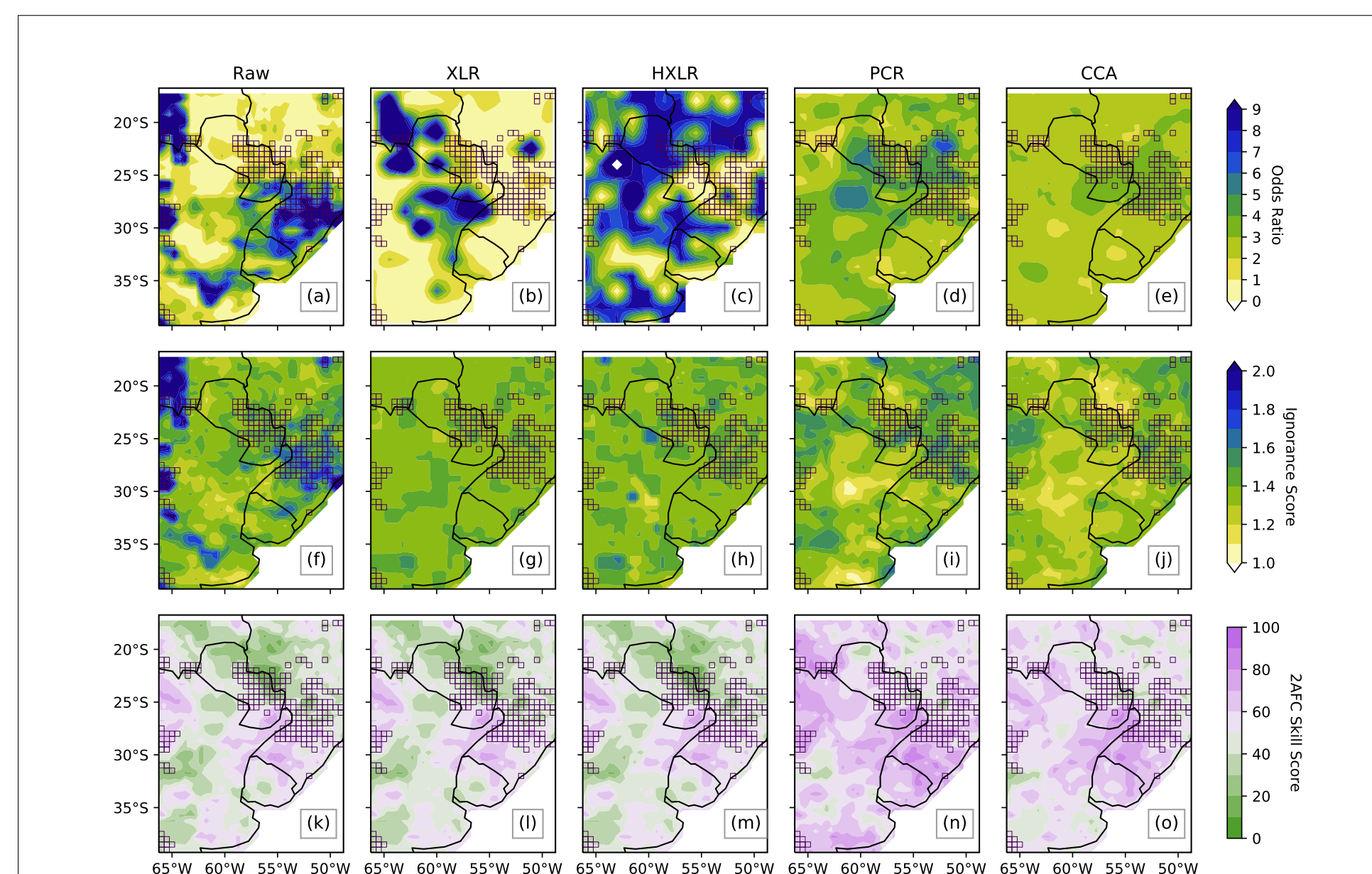

Figure 7: MOS-adjusted S2S model forecasts and skill scores. Top row shows the heavy rainfall (>90th percentile exceedance) forecast for 1-7 December 2015 as the odds ratio relative to climatology odds $= \frac{p}{1-p} \frac{1-p_c}{p_c}$. Second row shows the Ignorance score IGN $= -\log_2 p(Y)$. Bottom row shows the 2AFC skill score for each grid cell. For all three rows, the grid cells which experienced a 90th percentile exceedance for 1-7 December 2015 are outlined in black.

ENSO, MJO, and Weather Types

Figure 8: Anomalous probability of occurrence of each weather type concurrent with observance of each MJO and ENSO phase. Only values which are significant at $p < 0.10$ are shown.
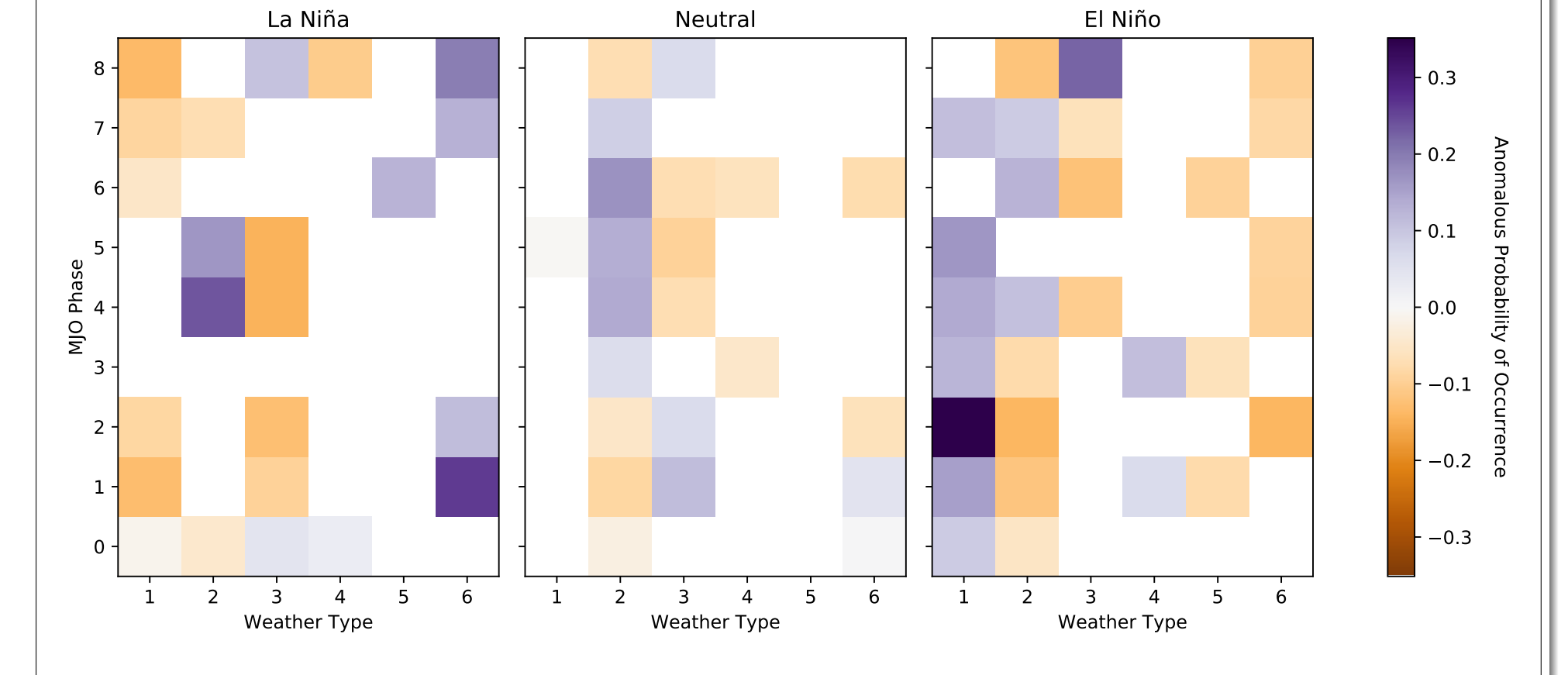
WT 1 occurs more frequently during El Niño years for most Madden-Julian Oscillation (MJO) phases, particularly during phase 2. During El Niño years, WT 3 - associated with dryness over the LPRB - occurs less frequently during MJO phases 4, 6, and 7, and more often during MJO phase 8; this is consistent with the lack of WT 3 during December 2015 and the frequent WT 3 occurrence in mid-January 2016 (fig. 3).

Atlantic-Pacific Interaction and WT4

While the occurrence of WT1 during NDJF 2015-16 is well explained by ENSO and MJO variability, these features alone do not explain the occurrence of WT4, the "No-Chaco" jet event. Previous studies emphasize the importance of Pacific-Atlantic interaction for forecasting climate effects in this region [13]. A persistent SST dipole in the central southern Atlantic Ocean favors the occurrence of WT4 by blocking transient extratropical wave activity coming from the Pacific, facilitating transitions from Chaco jet events (WT 1) to No-Chaco jet events (WT 4) via enhanced low-level wind circulation from southern Brazil towards the Atlantic, and back to north-east Brazil and the Amazon (see fig. 9). Composite analysis (not shown) of months with many WT4 occurrences is consistent with the schematic shown here.
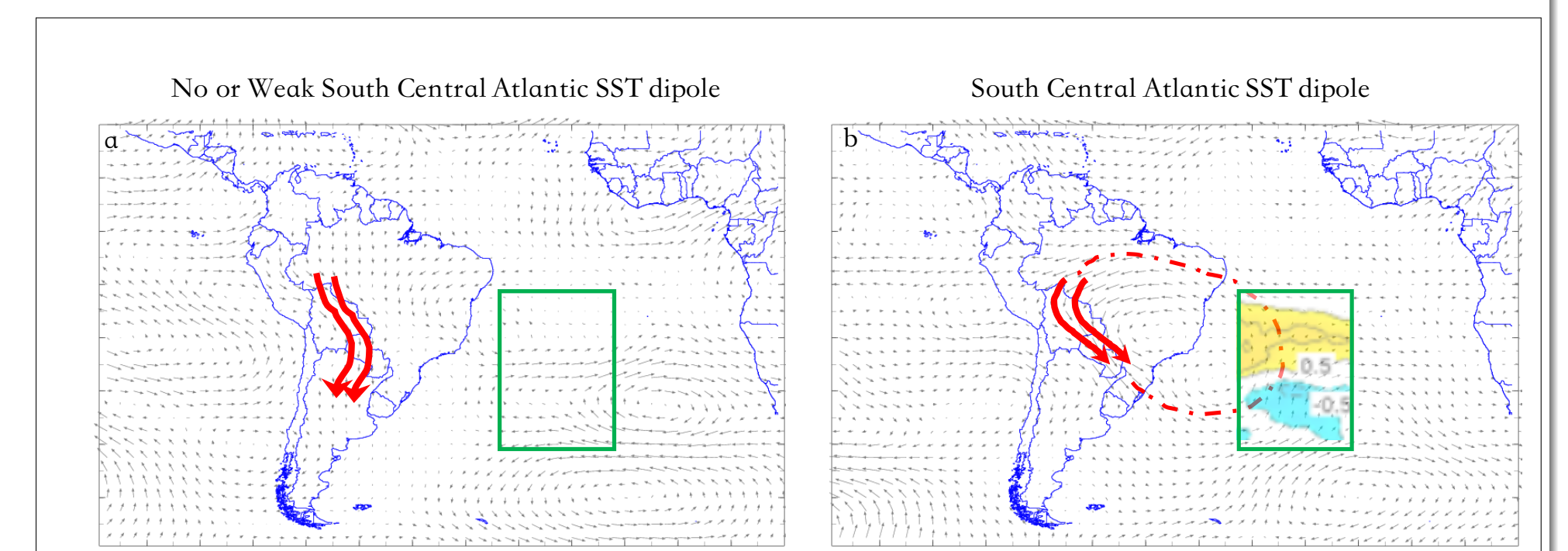

Figure 9: Schematics of low-level jet events (red arrows) during austral summer of El Niño years.

References

[1] J. A. Marengo et al. *Journal of Climate* (2004). [2] C. Vera et al. *Bulletin of the American Meteorological Society* (2006). [3] P. Xie et al. (1996). [4] M. Kanamitsu et al. *Bulletin of the American Meteorological Society* (2002). [5] Á. G. Muñoz et al. *Journal of Climate* (2015). [6] A. Dawson. *Journal of Open Research Software* (2016). [7] P. A. Michelangeli et al. *Journal of the Atmospheric Sciences* (1995). [8] P. Salio et al. (2002). [9] V. R. Barros et al. *Journal of Hydrometeorology* (2004). [10] J. M. Bravo et al. *Journal of Hydrologic Engineering* (2012). [11] G. W. Carbin et al. *Bulletin of the American Meteorological Society* (2016). [12] H. R. Glahn and D. A. Lowry. *Journal of Applied Meteorology* (1972). [13] M. Barreiro. *International Journal of Climatology* (2017).